THE JOURNAL OF BIOLOGICAL CHEMISTRY VOL. 286, NO. 36, pp. 31598–31609, September 9, 2011

ZF21 Protein, a Regulator of the Disassembly of Focal Adhesions and Cancer Metastasis, Contains a Novel Noncanonical Pleckstrin Homology Domain*[S]

Received for publication, November 1, 2010, and in revised form, July 9, 2011 Published, JBC Papers in Press, July 15, 2011, DOI 10.1074/jbc.M110.199430

Makoto Nagano[‡§1], Daisuke Hoshino[‡1], Seizo Koshiba[¶‖], Takuya Shuo[‡], Naohiko Koshikawa[‡], Tadashi Tomizawa[¶], Fumiaki Hayashi[¶], Naoya Tochio[¶], Takushi Harada[¶], Toshifumi Akizawa[§], Satoru Watanabe[¶], Noriko Handa[¶], Mikako Shirouzu[¶], Takanori Kigawa[¶], Shigeyuki Yokoyama[¶‡‡], and Motoharu Seiki[‡2]**

*From the [‡]Division of Cancer Cell Research, Institute of Medical Science, University of Tokyo, Minato-ku, Tokyo, 108-8639, the [§]Faculty of Pharmaceutical Sciences, Setsunan University, 45-1 Nagaotogecho, Hirakata Osaka, 573-0101, the [¶]RIKEN Systems and Structural Biology Center, Yokohama Institute, 1-7-22 Suehiro-cho, Tsurumi, Yokohama 230-0045, the [‖]Department of Supramolecular Biology, International Graduate School of Arts and Sciences, Yokohama City University, 1-7-29 Suehiro-cho, Tsurumi, Yokohama 230-0045, the **Department of Computational Intelligence and Systems Science, Interdisciplinary Graduate School of Science and Engineering, Tokyo Institute of Technology, 4259 Nagatsuda-cho, Midori-ku, Yokohama 226-8502, and the [‡‡]Department of Biophysics and Biochemistry, Graduate School of Science, The University of Tokyo, 7-3-1 Hongo, Bunkyo-ku, Tokyo 113-0033, Japan*

Directional migration of adherent cells on an extracellular matrix requires repeated formation and disassembly of focal adhesions (FAs). Directional migration of adherent cellsWe have identified ZF21 as a regulator of disassembly of FAs and cell migration, and increased expression of the gene has been linked to metastatic colon cancer. ZF21 is a member of a protein family characterized by the presence of the FYVE domain, which is conserved among Fab1p, YOPB, Vps27p, and EEA1 proteins, and has been shown to mediate the binding of such proteins to phosphoinositides in the lipid layers of cell membranes. ZF21 binds multiple factors that promote disassembly of FAs such as FAK, β-tubulin, m-calpain, and SHP-2. ZF21 does not contain any other known protein motifs other than the FYVE domain, but a region of the protein C-terminal to the FYVE domain is sufficient to mediate binding to β-tubulin. In this study, we demonstrate that the C-terminal region is important for the ability of ZF21 to induce disassembly of FAs and cell migration, and to promote an early step of experimental metastasis to the lung in mice. In light of the importance of the C-terminal region, we analyzed its ternary structure using NMR spectroscopy. We demonstrate that this region exhibits a structure similar to that of a canonical pleckstrin homology domain, but that it lacks a positively charged interface to bind phosphatidylinositol phosphate. Thus, ZF21 contains a novel noncanonical PH-like domain that is a possible target to develop a therapeutic strategy to treat metastatic cancer.

Interaction between cells and extracellular matrices (ECM)[3] plays crucial roles during physiological processes such as embryonic development, wound repair, angiogenesis, and pathological processes such as cancer metastasis (1–4). Integrins act as major receptors for ECM proteins and transmit bidirectional transmembrane signals upon binding to the latter (5). Binding to the ECM causes integrins to cluster, which leads to the recruitment of various cellular proteins to the inner surface of the plasma membrane so as to form structures called focal adhesions (FA) (5, 6). The cytoplasmic proteins recruited to the cytoplasmic portion of integrins at FAs include signal proteins, such as focal adhesion kinase (FAK) and c-Src, and adaptor proteins, such as paxillin, vinculin, talin, α-actinin, and p130Cas (7–9). Some FA components, such as talin and vinculin, are further linked to the actin cytoskeleton and allow the generation of the forces that maintain cell morphology and mediate cell migration via the contraction of actin fibers (10, 11). However, a dynamic turnover of FAs is necessary for cell migration and the processes triggering the formation and disassembly of FAs are regulated by distinct mechanisms, although the details of these mechanisms remain to be clarified (12).

The formation of FAs has been studied extensively. On the other hand, the process of FA disassembly remains unclear, although several proteins that play specific roles during the disassembly step have been identified (13, 14). Microtubules (MTs) are key regulators that initiate disassembly of FAs (12, 15, 16). Treatment of cells with nocodazole, an agent that disrupts MTs, stabilizes FAs, and subsequent depletion of the agent releases the blockade allowing disassembly of FAs to resume in a synchronous manner (12, 15, 16). FAK, especially the form phosphorylated at Tyr^{397}, is required to internalize

* This work was supported by a Grant-in-Aid for Scientific Research (S) and Core Research for Evolutional Science and Technology (CREST) (to M. S.), the RIKEN Structural Genomics/Proteomics Initiative (RSGI), and the National Project on Protein Structural and Functional Analyses (to S. Y.) from the Ministry of Education, Culture, Sports, Science, and Technology of Japan.

[S] The on-line version of this article (available at http://www.jbc.org) contains supplemental Table S1 and Figs. S1–S5.

[1] Both authors contributed equally to this work.

[2] To whom correspondence should be addressed: 4-6-1 Shirokanedai, Minato-ku, Tokyo 108-8639, Japan. Fax: 81-3-5449-5414; E-mail: mseiki@ims.u-tokyo.ac.jp.

[3] The abbreviations used are: ECM, extracellular matrix; EEA1, early endosome antigen 1; FA, focal adhesion; FYVE, Fab1p YOPB Vps27p EEA1; MT, microtubule; m1V, m1Venus; PH, pleckistrin homology; PI(3)P, phosphatidylinositol 3-phosphate; ZF21, ZFYVE21; C-ter, C-terminal; aa, amino acid(s); $Ins(1,4,5)P_3$, inositol (1,4,5)-trisphosphate; PLC, phospholipase C.

integrin β1 from the surface by recruiting dynamin to FAs (12). Calpain-1 and -2, classical members of the family of calcium-dependent endopeptidases, are also crucial for the MT-mediated disassembly of FAs by cleaving components such as integrin, FAK, paxillin, talin, and α-actinin (17). Dephosphorylation of FAK, paxillin, and p130Cas by protein tyrosine phosphates, such as PTP-PEST, SHP-2, or PTP-1B, also induces the disassembly of FAs (18–20). However, further information is needed to understand how these factors coordinate FA disassembly.

We have recently been studying functions of cytoplasmic adaptor proteins that are localized in close proximity to the invasion-promoting membrane protease, MT1-MMP (21–25). These include MTCBP-1, which regulates cell migration by unknown mechanisms (21); Mint3, which regulates activation of HIF-1α via the cytoplasmic tail of MT1-MMP (23, 25); p27RF-Rho (LAMTOR1), which regulates formation of invadopodia (26); and ZF21 (MTCBP-2), which regulates the disassembly of FAs (27, 28). ZF21 is expressed ubiquitously in adherent cells and contains an FYVE domain (29), which binds phosphoinositides in the lipid layers of cell membranes. It localizes predominantly to endosomes, but is also found in FAs at the ECM-cell interface. Depletion of ZF21 expression by RNA interference prevents disassembly of FAs, increases the adherence of cells to the ECM, and reduces cell migration. Depletion of ZF21 does not affect the extent of accumulation of FAs in cells treated with nocodazole, but specifically prevents disassembly of FAs after removal of nocodazole. The results indicate that ZF21 is required during MT-dependent disassembly of FAs. Using pulldown or immunoprecipitation assays, we also found that ZF21 binds the above mentioned disassembly related proteins, such as FAK, SHP-2, m-calpain, and β-tubulin (27, 28). Therefore, it is conceivable that ZF21 associated with vesicles being transported by microtubules via its FYVE domain may also carry SHP-2 and m-calpain on the vesicles. Because depletion of ZF21 in cells prevents dephosphorylation of FAK at FAs, ZF21 may deliver SHP-2 to FAK so as to facilitate the dephosphorylation of the latter. These FA-disassembly proteins interact with ZF21 through the FYVE domain and other regions of the protein. For example, the FYVE domain and the region C-terminal to the FYVE domain are sufficient to bind FAK and β-tubulin, respectively (27). Although the FYVE domain is conserved among family members, the N- and C-terminal regions of ZF21 show no similarity to other known proteins. Therefore, distinct protein-protein interaction interfaces that are independent from the FYVE domain appear to be important in the function of ZF21.

In this study, we evaluate the contribution of each region of the ZF21 protein to the disassembly of FAs and the promotion of cell migration. Furthermore, consistent with the fact that the expression of ZF21 is specifically enhanced in metastatic human colon carcinomas (30), we demonstrate that ZF21 indeed promotes an early step of metastasis of tumor cells to the lung in mice, in a fashion dependent upon both the FYVE domain and the C-terminal region of ZF21. In light of the importance of the C-terminal region of ZF21, we analyzed its ternary structure in solution using NMR spectroscopy. The C-terminal fragment contains a protein fold similar to that of the canonical pleckstrin homology (PH) domain (31) despite exhibiting no amino acid sequence homology to the latter. In addition, the PH-like domain of ZF21 appears to lack an interface to bind phospholipids. Thus, ZF21 contains a novel PH-like protein fold within the region C-terminal to the FYVE domain, and both this PH-like domain and the FYVE domain are important for mediating both disassembly of FAs and promotion of metastasis.

EXPERIMENTAL PROCEDURES

Cells, Antibodies, and Reagents—MDA-MB231 and HeLa cells were obtained from the American Type Culture Collection (Manassas, VA). Cells were cultured in DMEM (Invitrogen), supplemented with 10% fetal bovine serum, penicillin, and streptomycin (Invitrogen Corp.). All cells were cultured at 37 °C under a 5% CO_2, 95% air atmosphere. A polyclonal anti-ZF21 antibody was prepared as described previously. We used commercially available antibodies to detect GFP (Invitrogen), actin (C4, Millipore), FAK (BD Biosciences), and Tyr^{397}-phosphorylated FAK (BIOSOURCE). Nocodazole (Sigma) was used at 5 μM. All other chemical reagents were purchased from Sigma or Wako, unless otherwise indicated.

Plasmids—cDNAs encoding ZF21 or EEA1 were amplified from HT1080 cells by reverse transcription-PCR (RT-PCR). Expression constructs encoding ZF21-N (aa 1–105), ZF21-FYVE (aa 41–105), and EEA1-FYVE (aa 1349–1411) were prepared by RT-PCR using human *ZF21* and *EEA1* genes. The FYVE domain (encoded by aa 41–103) of the ZF21 mutant (SWAP) is replaced by the FYVE domain from EEA1 (encoded by aa 1349–1411). The mammalian expression vector pLenti6/V5-DEST or the *Escherichia coli* expression vector pDEST15 (Invitrogen) was used to express the recombinant proteins as described previously.

Knockdown Experiments Using shRNA—The coding sequence of the shRNA used to knock down human ZF21 expression is as follows: 5′-caccgcagtgtgacgccaagtttgacgaatcaaacttg-gcgtcacactgc-3′. The sequence of the shRNA used to knock down expression of human FAK is as follows: 5′-caccgcatcttc-cagttacaaattccgaagaatttgtaactggaagatgc-3′ (shFAK#1). Lentiviral vectors expressing the shRNAs were generated and used according to the manufacturer's instructions. For rescue of ZF21 expression following shRNA-mediated knockdown, an expression construct encoding a mutant ZF21 mRNA refractory to the shRNA was generated by site-directed mutagenesis and the mutant protein was expressed with a m1Venus tag at the N terminus, using the pENTR vector (Invitrogen).

Cell Migration Assay—The transwell migration assay was performed as described previously (28). Briefly, both sides of transwells with 8-μm pore size filters (Corning) were precoated with fibronectin (5 μg/ml). DMEM containing 10% FBS was added to the lower chamber, and a cell suspension (5×10^4 cells) was placed in the upper chamber. Following incubation for 6 h, the cells that had migrated to the lower chamber were stained with 0.5% crystal violet solution and counted using a light microscope at ×200 magnification. Values represent averages from 5 fields.

Pulldown Assay—The pulldown assay was performed as described previously (28). Briefly, cleared cell lysates were incubated with GST-tagged ZF21 (GST-WT) or the ZF21 mutant

that had been previously bound to glutathione-conjugated Sepharose beads at 4 °C for 6 h. Pellets containing the beads were collected, washed with RIPA buffer used for cell lysis, and subjected to SDS-PAGE followed by Western blot analysis using the indicated antibodies.

Focal Adhesion Disassembly Assay—The focal adhesion disassembly assay was performed as described previously (28). Briefly, cells were grown on fibronectin-coated glass coverslips and treated with 5 μM nocodazole for 30 min to depolymerize microtubules. After the drug was removed, cells were incubated to resume polymerization of microtubules. Cells were fixed in −20 °C methanol for 10 min, rehydrated in PBS followed by permeablization with 0.1% Triton X-100 in PBS for 5 min, and subjected to immunostaining.

FAK Dephosphorylation Assay—The FAK dephosphorylation assay was performed as described previously (28). Briefly, cells were grown on fibronectin-coated plastic dishes and treated with 5 μM nocodazole for 30 min to depolymerize microtubules. After the drug was removed, cells were incubated to resume polymerization of microtubules. Cells lysates were resolved by PAGE following cell lysis and mixing with Laemmli sample buffer and the extent of FAK phosphorylation was evaluated by Western blot analysis.

Protein Expression and Purification for the Structural Analysis—The C-terminal region of zinc finger FYVE domain-containing protein 21 (ZF21) (amino acid residues Ala^{107} to Gln^{234}) (Swiss-Prot code Q9BQ24) was cloned into the expression vector pCR2.1 (Invitrogen), as a fusion with an N-terminal His_6 affinity tag and a tobacco etch virus protease cleavage site (32). The actual construct contains seven extra residues (GSSGSSG) after the tobacco etch virus cleavage site and six extra residues at the C terminus (SGPSSG) derived from the expression vector. The fusion protein was synthesized using a cell-free protein expression system and $^{13}C/^{15}N$-labeled amino acids (33, 34), and was subsequently purified using a chelating column, as described elsewhere (35). The purified protein was concentrated to 1.2 mM in 20 mM $^2H_{11}$ Tris-HCl buffer (pH 7.0), containing 100 mM NaCl, 1 mM $^2H_{10}$ dithiothreitol, 10% ^2H_2O, and 0.02%(w/v) NaN_3.

Structure Determination—All NMR experiments were performed at 296 K on Bruker 600- and 900-MHz Avance spectrometers, and on Varian 600-, 800-, and 900-MHz Inova spectrometers. Resonance assignments were accomplished using standard NMR techniques, as described elsewhere (35). NMR spectra acquired for the assignments and distance restraints were two-dimensional ^1H-^{15}N HSQC, ^1H-^{13}C HSQC, three-dimensional HNCA, HN(CO)CA, HNCO, (HCA)CO(CA)NH, HNCACB, CBCA(CO)NH, HBHANH, C(CCO)NH, HC(C)H-TOCSY, (H)CCH-TOCSY, HNHB, HN(CO)HB, ^{15}N-edited NOESY-HSQC (60 ms mixing time), and ^{13}C-edited NOESY-HSQC (50 ms mixing time). All of the spectra were processed using the program NMRPipe (36). Analyses of the processed data were performed with the programs NMRView and KUJIRA (37, 38).

Automated NOE cross-peak assignments and structure calculations with torsion angle dynamics were performed using the CYANA software package (39, 40). Two NOE peak lists, obtained from three-dimensional ^{15}N-edited NOESY-HSQC and ^{13}C-edited NOESY-HSQC spectra, were used for structure calculations. In addition, backbone dihedral angle restraints, derived from the program TALOS, were used for structure calculations (41). A total of 100 structures were independently calculated, and the 20 structures in the final calculation cycle with the lowest target function values were selected. The structures were validated using the program PROCHECK-NMR (42). The programs MOLMOL (43) and PyMOL (DeLano Scientific, Palo Alto, CA) were used for analyzing the calculated structures and preparing the drawings of the structures.

Lung Colonization Assays—The lung colonization assays used cells fluorescently labeled with CellTracker Green and CellTracker Orange (Invitrogen). ZF21-depleted and control cells, ZF21-depleted cells, and HT1080 cells (1×10^5 each for HT1080 and MDA-MB231) were injected into the tail veins of nude mice, which were killed 1 or 24 h later. Fluorescently labeled cells in the lung were counted by confocal microscopy (Nikon).

RESULTS

FAK Binds the FYVE Domain of ZF21 but Not EEA1—The domain structures of ZF21 and EEA1 and the regions of the proteins interacting with protein factors are shown schematically in Fig. 1*A*. The FYVE domain and the C-terminal region (C-ter) of ZF21 are sufficient to bind FAK and β-tubulin, respectively (28). In contrast, both the N-terminal fragment including the FYVE domain (N-ter + FYVE) and the C-terminal region are required for binding m-calpain (28) or SHP-2 (supplemental Fig. S1). Unlike ZF21, the FYVE domain of EEA1 is located at the C terminus and in contrast to ZF21, its binding proteins have not been implicated in FA disassembly (Fig. 1*A*). ZF21 localizes to FAs as expected from its binding to FAK (Fig. 1*B*, *a*) and also associates with endosome vesicles through interaction with PI(3)P via the FYVE domain (Fig. 1*B*, *b*). Mutations in the FYVE domain abolish localization of ZF21 to endosomes and abrogate the ability of the protein to promote cell migration, as demonstrated previously (27). The interaction of ZF21 with FAK also plays a pivotal role in cell migration, as evidenced by the fact that ZF21 cannot promote cell migration in MDA-MB231 cells in which the endogenous FAK has been depleted by expression of shRNA (Fig. 1*C*, and supplemental Fig. S2 for protein expression levels).

Members of the FYVE domain-containing family of proteins contain two conserved zinc fingers and basic amino acid residues. Comparison of the FYVE domain sequences of ZF21 and EEA1 reveals 41% overall amino acid conservation as shown in Fig. 2*A*. Therefore, we tested whether the FYVE domain sequence of EEA1 could bind FAK in a pulldown assay. We first generated a number of fusion proteins comprising glutathione *S*-transferase (GST) fused to the N termini of the FYVE domains of ZF21 or EAA1, or to full-length ZF21 or a mutant of the latter with its FYVE domain substituted by that of EEA1, as shown in Fig. 2*B*. These fusion proteins were used to pull down FAK from the HeLa cell lysate (Fig. 2*C*). The GST fusions to full-length ZF21 (GST-WT) or its FYVE domain alone (GST-ZF21FYVE) bound to FAK. In contrast, the GST fusions to the FYVE domain of EEA1 (GST-EEA1FYVE) or the FYVE

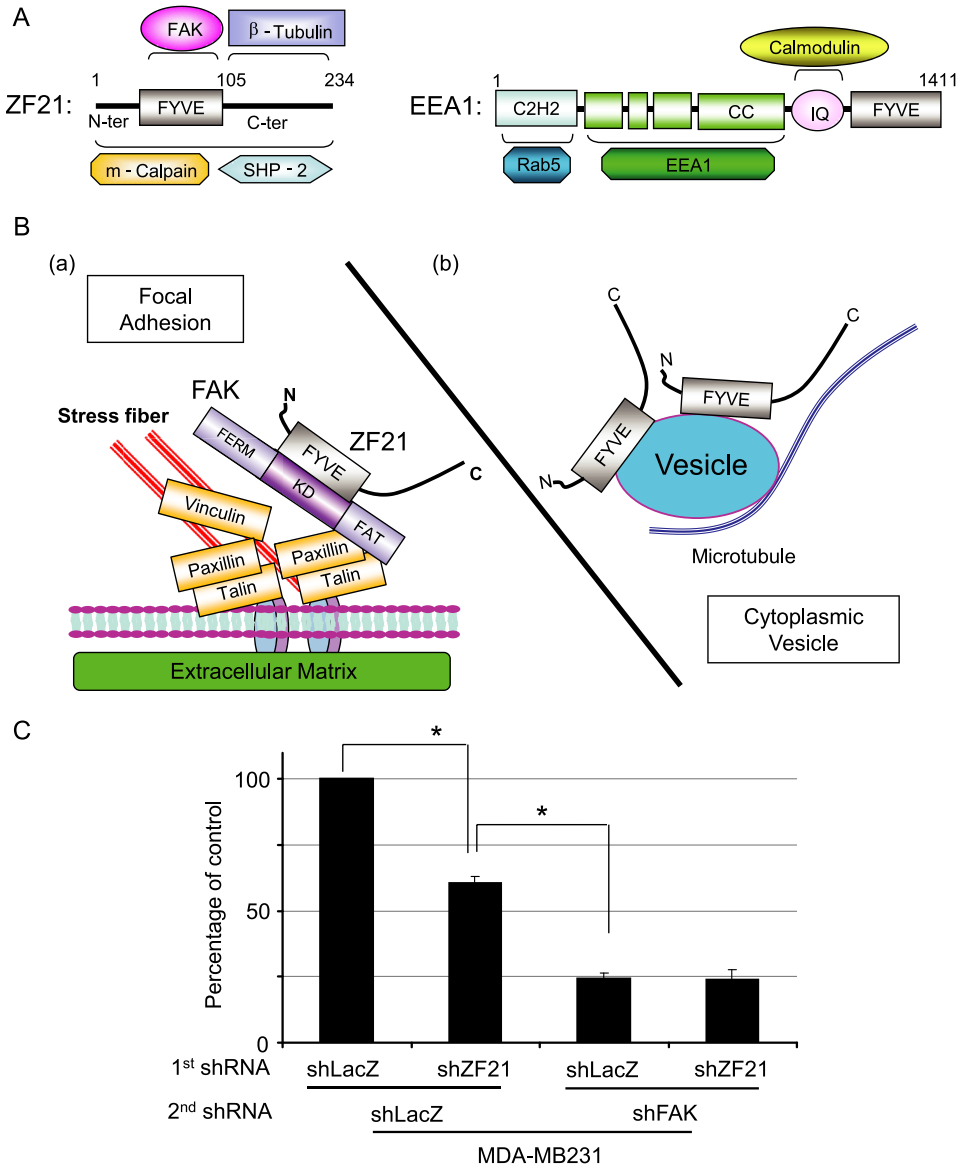

FIGURE 1. **ZF21 is an adaptor protein that regulates disassembly of FAs and migration of cells.** *A,* schematic illustration of the domain structures of ZF21 (*left*) and EEA1 (*right*). Binding proteins and regions of the respective proteins that interact with them are indicated. *B*, ZF21 resides in FAs (*a*) and on cytoplasmic vesicles (*b*). ZF21 binds to FAK and vesicles via the N-terminal FYVE domain. *C*, effect of FAK on ZF21-dependent cell migration was analyzed using MDA-MB-231 cells. Expression of either or both ZF21 and FAK was carried out by expressing the corresponding shRNAs. Knock down efficiency is presented under supplemental Fig. S2. Cells were subjected to a migration assay using a transwell chamber equipped with filters coated with fibronectin, and FBS was used as the attractant. *First lane,* shLacZ + shLacZ; *second lane,* shZF21 + shLacZ; *third lane,* shLacZ + shFAK; *fourth lane,* shZF21 + shFAK. *Error bars* represent the mean ± S.D. ($n = 3$). *, $p < 0.005$ (Student's *t* test).

domain-swapped ZF21 mutant (GST-SWAP) bound FAK very weakly.

Crucial Roles for the FYVE Domain and the C-terminal Region of ZF21 in Regulation of FAs and Cell Migration—To evaluate the contributions of the FYVE domain and the C-ter of ZF21 to the process of disassembly of FAs and the migratory activity of cells, we expressed the fusion proteins shown in Fig. 3*A* in human breast carcinoma MDA-MB-231 cells. These fusion proteins comprise an m1Venus tag fused to either full-length ZF21 (m1V-WT), the mutant ZF21 containing the FYVE domain of EEA1 (m1V-SWAP), or the fragment of ZF21 lacking the C-terminal region (m1V-N). These fusion proteins were individually expressed in MDA-MB-231 cells in which the expression of endogenous ZF21 was first depleted by expressing an shRNA targeting endogenous ZF21 (Fig. 3*B*). The exogenously expressed proteins are encoded by mRNAs resistant to the shRNA targeting endogenous ZF21. Disassembly of FAs was analyzed by treating the cells with nocodazole, which inhibits disassembly of FAs by disrupting microtubules. Subsequent deprivation of the drug from the culture medium induces disassembly of FAs in a synchronized manner. The FAs in MDA-MB231 cells in which expression of endogenous ZF21 was knocked down with shZF21 (MDA-MB231/shZF21) were visualized by monitoring the phosphorylated form of FAK at Tyr^{397} (Fig. 3*C*, *red*). In the control MDA-MB231/shZF21 cells, a significant number of FAs remained even 30 min following removal of nocodazole from the medium (Fig. 3*C*, 30 min/mock, *red*). In contrast, expression of m1V-WT in the cells

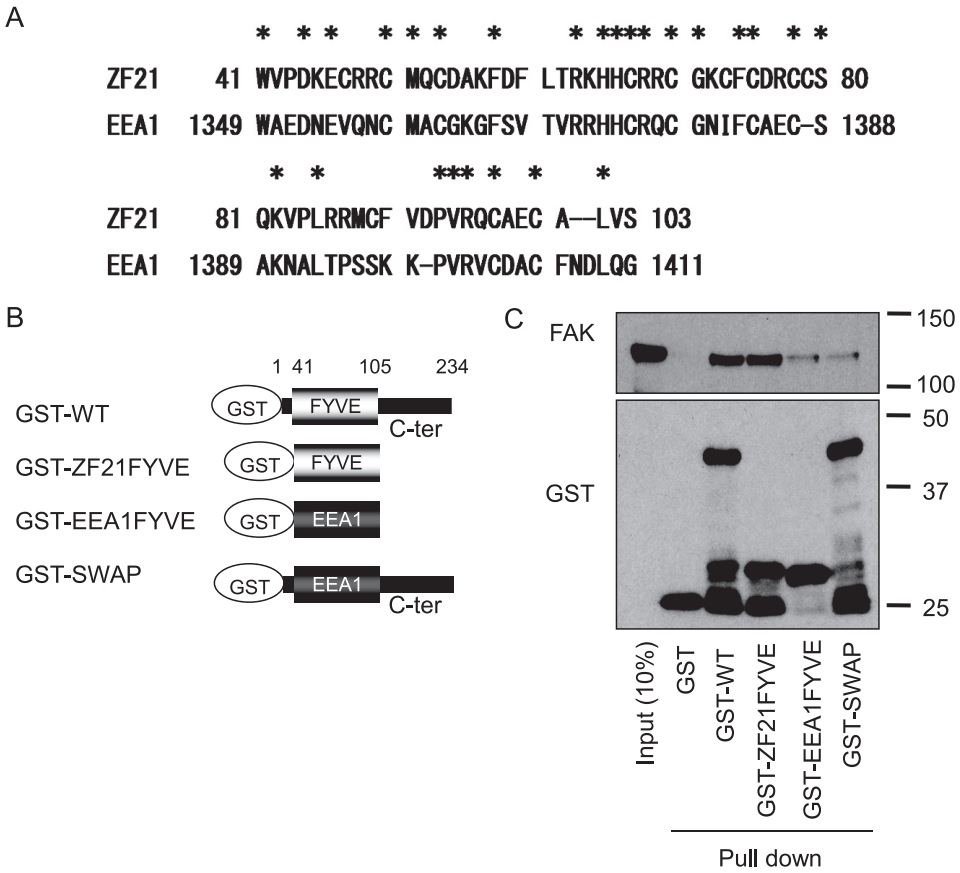

FIGURE 2. **The FYVE domain of ZF21 binds specifically to FAK.** *A*, sequence alignment of the FYVE domains of ZF21 and EEA1. Conserved residues are denoted with *asterisks*. *B*, schematic representation of the GST fusion proteins used for the FAK pulldown assay. GST was fused at the N terminus of wild-type ZF21 (GST-WT), the FYVE domain of ZF21 (GST-ZF21FYVE), the FYVE domain of EEA1 (GST-EEA1FYVE), or two full-length ZF21 that has had its FYVE domain substituted by that of EEA1 (GST-SWAP). The *numbers* in the figure represent amino acid positions. *C*, whole cell lysates of HeLa cells were incubated with GST-tagged ZF21 derivatives or GST alone. Proteins bound to the GST fusion proteins were analyzed by Western blot using anti-FAK or anti-GST antibodies.

promoted disassembly of FAs markedly, such that the majority of the FA signals had disappeared by 30 min (Fig. 3*C*, 30 min/m1V-WT, *red*), whereas expression of m1V-SWAP or m1V-N did not (Fig. 3*C*, 30 min/m1V-SWAP and m1V-N, *red*). Expression of the ZF21 fusion proteins in the cells was confirmed by monitoring the signal from the m1Venus tag (Fig. 3*C*, *green*). m1V-WT exhibited a punctate distribution, consistent with its association with vesicles, whereas m1V-SWAP and m1V-N appeared to be localized diffusely throughout the cytoplasm (Fig. 3*C*, *green*). The number of FAs evaluated by immunostaining of the phosphorylated form of FAK correlated well with the overall levels of phosphorylation of FAK at Tyr^{397} in the cells, as demonstrated by Western blot analysis (Fig. 3*D*). Merged pictures of the signals from both phospho-Tyr^{397}-FAK and the m1Venus tag are represented under supplemental Fig. S3.

We have previously reported that the rate of turnover of FAs regulated by ZF21 correlates with the migratory activity of cells and that the FYVE domain is indispensable for the activity (28). We next examined whether the mutant ZF21 proteins listed in Fig. 3*A* retain the ability to restore migration in ZF21-depleted cells using a transwell migration assay (Fig. 3*E*). As we reported previously, depletion of ZF21 (*second lane,* -/shZF21) decreased the migratory activity of cells relative to that of the control cells (*first lane,* -/shLacZ). Only the cells expressing m1Venus-tagged ZF21 (*fourth lane,* m1V-WT/shZF21) were able to migrate to an extent similar to that of the control cells (*first lane,* -/shLacZ), whereas the expression of the empty vector (*third lane,* mock), the mutant ZF21 containing the FYVE domain of EEA1 (m1V-SWAP), or the fragment of ZF21 lacking the C-terminal region (m1V-N) did not. Thus, both the FYVE domain and the C-ter region are indispensable for the regulation of FA disassembly and cell migration by ZF21.

Effect of the ZF21 on an Early Step of Experimental Metastasis to Lung—Increased migratory activity is a characteristic of highly metastatic tumor cells. Interestingly, the expression of ZF21 is increased in metastatic colorectal carcinomas, according to the results of serial analysis of gene expression analysis of clinical specimens (30). Therefore, we next evaluated the effect of the expression of ZF21 or the various truncation mutants on the metastatic ability of human tumor cells in mice. Tumor cell functions such as migration and invasion are important for metastatic spreading of tumors and formation of secondary colonies. For example, in an early step of lung metastasis, tumor cells that have reached the lung microvasculature must traverse the vessel wall for extravasation and establishment of an initial deposition in the lung parenchyma (44, 45). Therefore, we evaluated whether ZF21 affected an early step of experimental metastasis to the lung using MDA-MB231 cells and human fibrosarcoma HT1080 cells. Control (expressing shLacZ) and

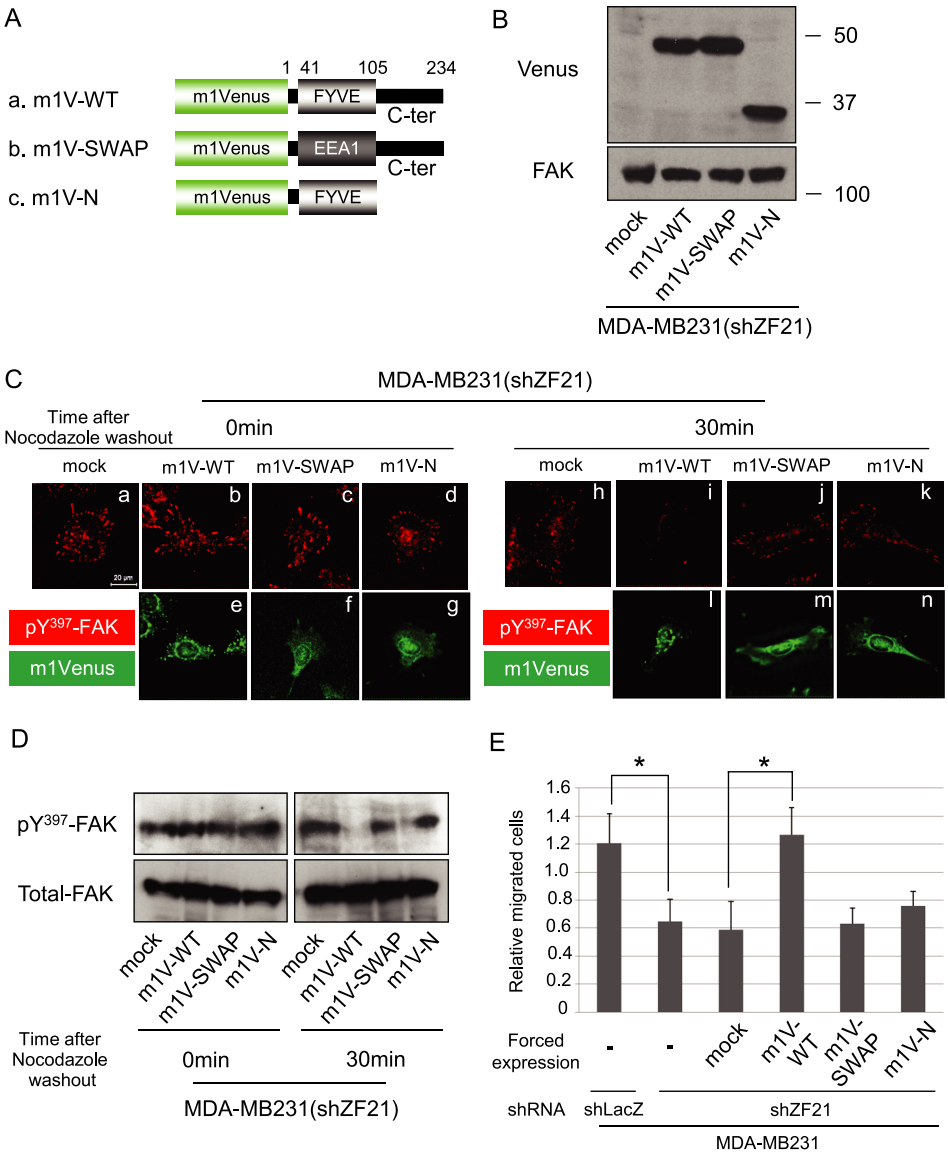

FIGURE 3. **Analysis of the contribution of regions of the ZF21 protein required for FA disassembly and promotion of cell migration.** *A*, schematic representation of the structures of the m1Venus-tagged fusion proteins of ZF21 expressed in ZF21-depleted MDA-MB231 cells (MDA-MB231(shZF21)). m1Venus was fused to the N terminus of wild-type ZF21 (*m1V-WT*), full-length ZF21 that has had its FYVE domain substituted by that of EEA1 (*m1V-SWAP*), or a ZF21 mutant lacking the C-terminal aa 106–234 region (*m1V-N*). *B*, each construct was stably expressed in MDA-MB231(shZF21) cells using a lentivirus vector system. The expression of each m1Venus-tagged protein was analyzed by Western blot using the indicated antibodies. The control (*mock*) represents cells infected with the empty lentiviral vector. *C*, immunostaining of MDA-MB-231(shZF21) cells for phospho-Tyr^{397}-FAK. MDA-MB231(shZF21) cells were seeded onto fibronectin-coated glass coverslips and cultured for 48 h. The cells were treated with nocodazole (5 μM) for 30 min. Then the cells were washed and cultured with nocodazole-free media for 0 (*a–g*) or 30 min (*h–n*). The cells were subjected to immunostaining for phospho-Tyr^{397}-FAK (*red*, *a–d* and *h–k*). ZF21 or the mutant thereof was visualized using the fluorescence of the tagged m1Venus protein (*green*, *e–g* and *l–n*). *Scale bar*, 20 μm. *D*, the same set of cells used in *C* was subjected to Western blot analysis using specific antibodies to detect the indicated forms of FAK. *E*, the cells were subjected to a migration assay using a transwell chamber equipped with filters coated with fibronectin and FBS was used as an attractant. *First lane,* shLacZ alone; *second lane,* shZF21 alone; *third lane,* shZF21 + mock vector; *fourth lane,* shZF21 + m1V-WT; *fifth lane,* shZF21 + m1V-SWAP; *sixth lane,* shZF21 + m1V-N. *Error bars* indicate the mean ± S.D. ($n = 3$). *, $p < 0.005$ (Student's *t* test).

ZF21-depleted cells (expressing shZF21) were labeled with red and green fluorescent protein cell trackers, respectively, and a mixture of the cells was injected into the tail vein of mice. Effect of expression of the shRNAs in the cells was confirmed by Western blot analysis (supplemental Fig. S4, *A* and *B*). The number of cells that reached the lung was evaluated 1 and 24 h later (Fig. 4). A similar number of red and green circulating cells were observed to reach the lung 1 h after injection (Fig. 4, *A–C*, *1 h*). However, most circulating cells were cleared from the lung during the following 24 h and only a limited number of cells remained in the lung tissue at this time point (Fig. 4, *A* for MDA-MB231, and *B* for HT1080, *24 h*). These are presumably the cells that escaped from the bloodstream after extravasation. Comparison of control shLacZ (*red*) and shZF21 (*green*) cells showed that shLacZ cells were retained more frequently than shZF21 cells (Fig. 4*C*). Thus, ZF21 contributes to the metastatic ability of tumor cells, at least at an early step that reflects extravasation and survival of the cells.

Using the same assay system, we next assessed whether ZF21 or the mutants thereof (m1V-WT, m1V-SWAP, or m1V-N,

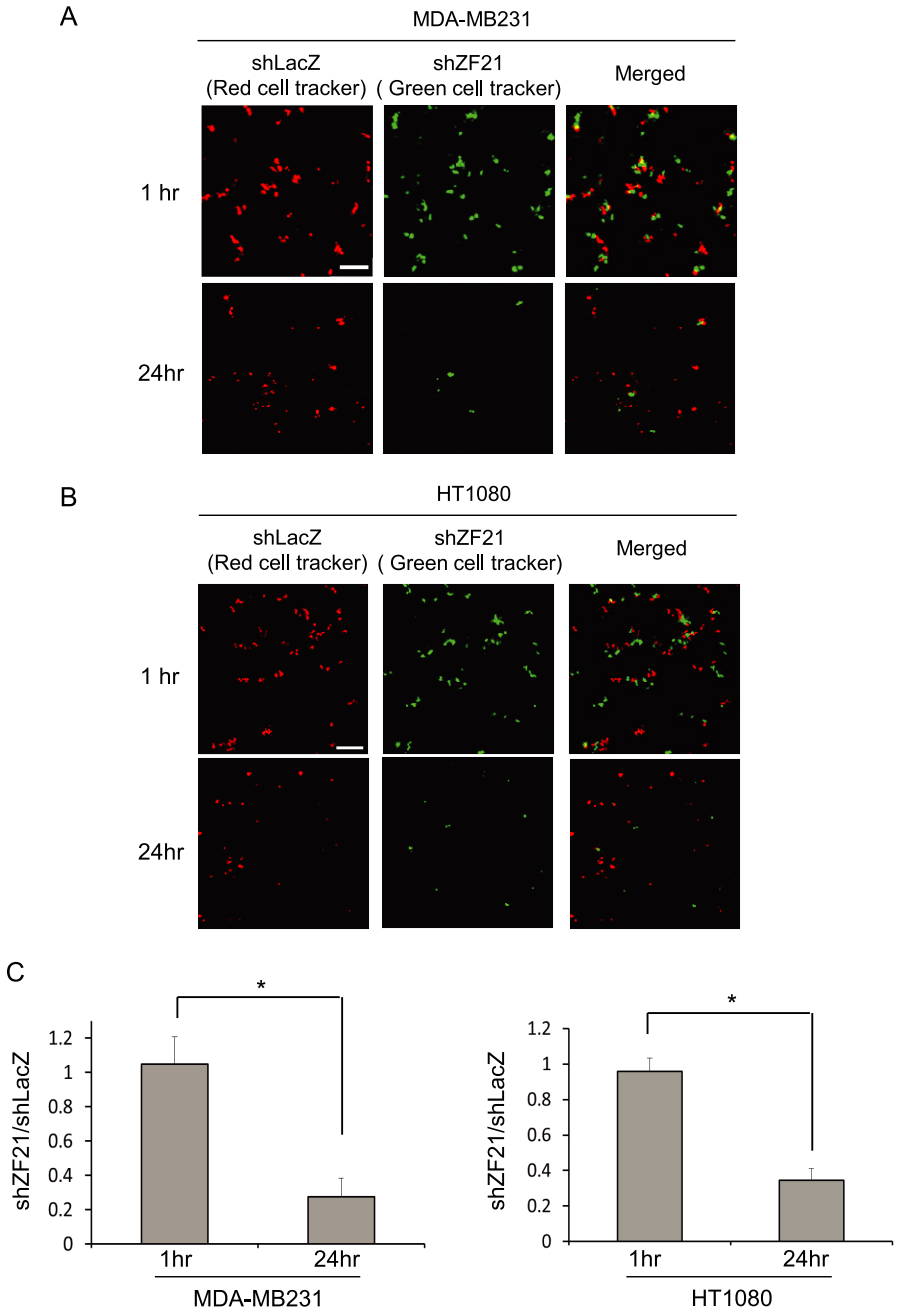

FIGURE 4. **ZF21 promotes an early step of metastasis of tumor cells to the lung.** As baseed on the reported methods (44, 45), metastasis of human tumor cells to the lung was analyzed by injecting the cells into the tail vein of mice. MDA-MB231 (*A*) or HT1080 (*B*) cells were used for the assay. Control cells were labeled with cell tracker *orange* and ZF21-depleted cells with cell tracker *green*. An equal number of the control and depleted cells were mixed and injected into the tail vein. The lung was dissected 1 or 24 h after injection and tumor cells in the tissue section were visualized (*A* and *B*) and the number of the cells counted (*C*). *Error bars* indicate the mean ± S.D. ($n = 3$). *, $p < 0.005$ (Student's *t* test).

summarized in Fig. 3*A*) could restore the metastatic activity of ZF21-depleted cells (Fig. 5). The ZF21-depleted cells expressing the empty vector (mock) or ZF21 mutants were labeled with green cell trackers. ZF21-depleted cells (expressing shZF21 alone) were labeled with red cell trackers. The green (mock, m1V-WT, m1V-SWAP, or m1V-N expressed in shZF21 cells) and red (shZF21 alone) labeled cells were mixed and injected into the tail vein of mice. One hour after injection, green-labeled cells were observed to reach the lung to an extent similar to that of the red-labeled cells (Fig. 5*A*). Only cells expressing the wild type ZF21 fusion (Fig. 5*B*, shZF21+m1V-WT, *green*) exhibited a greater rate of survival in the lung compared with the ZF21-depleted cells (Fig. 5*B*, shZF21, *red*), whereas cells expressing the other ZF21 fusions could not promote survival of the cells in the lung at 24 h after injection (Fig. 5*B*, shZF21 + mock, m1V-SWAP, or m1V-N, *green*). Indeed, the ZF21-depleted cells expressing m1V-WT formed metastatic colonies in lung at 5 weeks after injection, whereas those expressing either the m1V-SWAP or m1V-N did not (supplemental Fig. S5). Thus, both the FYVE domain and the C-ter of ZF21 are indispensable for the metastasis-promoting activity of ZF21.

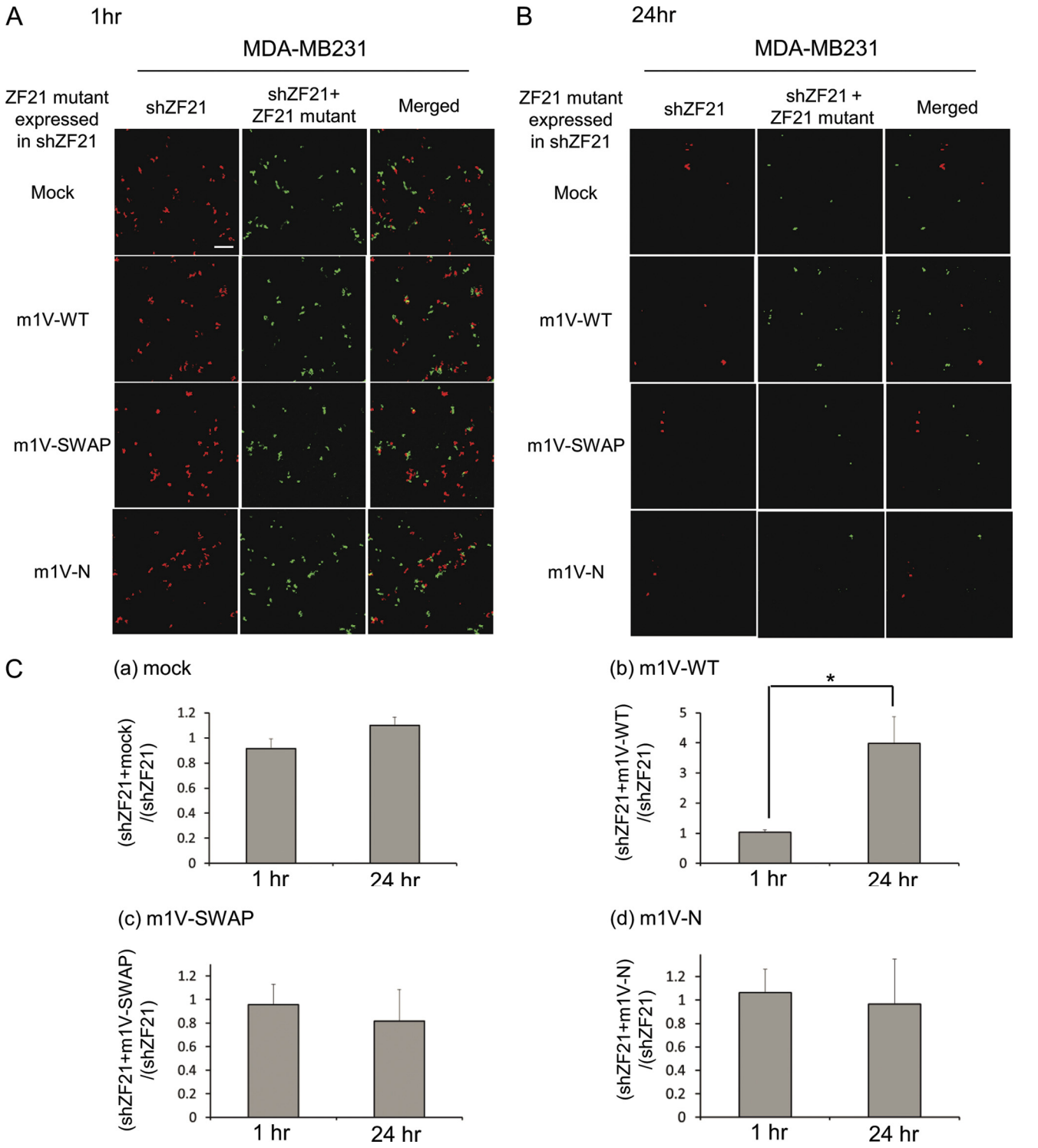

FIGURE 5. **Analysis of the contribution of the FYVE and the C-terminal domains to the activity of ZF21 in the experimental metastasis assay.** MDA-MB231 cells expressing shZF21 alone were labeled with *red* cell tracker and the cells expressing both shZF21 and each of the fusions shown in Fig. 3 were labeled with *green* cell tracker. A similar number of cells labeled with each color were mixed and analyzed as described in the legend to Fig. 4. Tissue sections analyzed at 1 (*A*) or 24 h (*B*) after injection are presented. The number of colored cells was counted and is presented in *C*. *Error bars* indicate the mean ± S.D. ($n = 3$). *, $p < 0.005$ (Student's *t* test).

The C-terminal Region of ZF21 Exhibits a Structural Fold Similar to That of Members of the PH Domain Superfold Family—The FYVE domain of ZF21 binds both PI(3)P and FAK. The sequence conservation between ZF21 and EEA1 within the FYVE domain indicates that the FYVE domain of ZF21 has a similar fold to the reported structure of EEA1 (46, 47). In contrast, the C-ter of ZF21 alone is sufficient to bind β-tubulin suggesting that the C-ter of ZF21 contains an independent protein fold.

To investigate the domain composition of the C-ter of ZF21, we first searched the Pfam data base (Pfam 24.0) with the

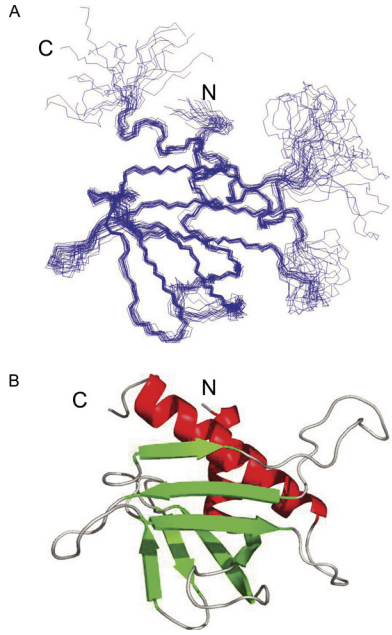

FIGURE 6. **Structures of the C-terminal domain of ZF21.** *A*, the ensemble of the final 20 best structures of the ZF21 C-terminal domain. The N and C termini are indicated as *N* and *C*, respectively. *B*, ribbon representation of the C-terminal domain is presented using a colored ribbon. The α-helices and β-strands are shown in *red* and *green*, respectively. The orientation is the same as in *A*.

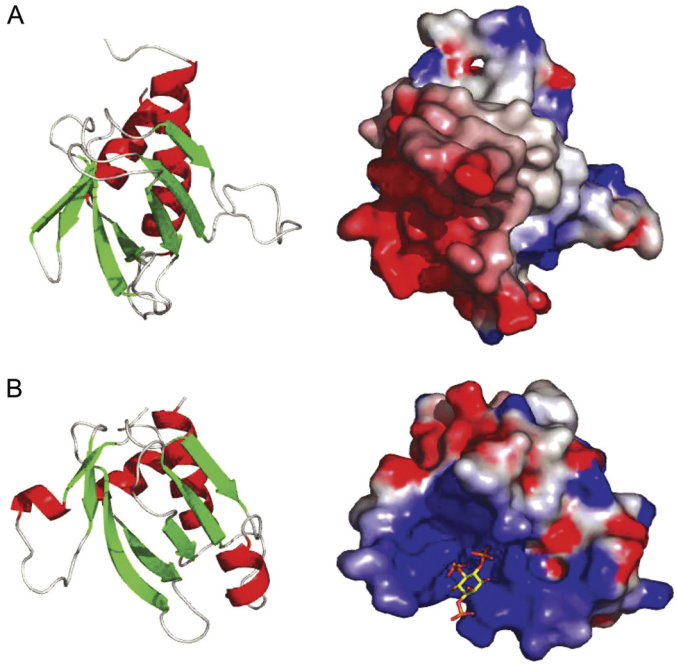

FIGURE 7. **Comparison of the structures of the ZF21 C-terminal and PLC-δ1 PH domains.** *A*, the ZF21 C-terminal domain. *B*, crystal structure of the PLC-δ1 PH domain in complex with Ins(1,4,5)P_3 (PDB code 1MAI). *Left panels* are ribbon representations. The α-helices and β-strands are shown in *red* and *green*, respectively. Ins(1,4,5)P_3 is shown as a *stick* model. *Right panels* are electrostatic potential surfaces. The electrostatic potentials were calculated with the GRASP program (58). The range of the potential is from −5.0 (*red*) to +5.0 kT/e (*blue*). The orientations are the same as in the *left panels*.

sequence of this region (48). However, we could not find any Pfam matches, indicating that this C-terminal region lacks sequence homology with known domains (data not shown). Hence, to elucidate the structure of the C-terminal region of ZF21, we used NMR spectroscopy to determine the solution structure of the C-ter fragment of ZF21 synthesized using an *in vitro* cell-free system. The structural statistics and the NMR constraints are summarized in supplemental Table S1. Fig. 6*A* shows the set of the 20 lowest energy structures of the C-terminal fragment of ZF21, and Fig. 6*B* shows a ribbon representation of a representative structure of the same fragment. The root mean square deviations for the C-ter fragment (Ala^{107}–Glu^{170}, Arg^{180}–Glu^{230}) are 0.83 ± 0.16 Å for the backbone atoms and 1.29 ± 0.14 Å for the heavy atoms, respectively.

The C-ter region of ZF21 adopts a compact, globular fold, which consists of seven β-strands (β1, Ala^{121}–Val^{125}; β2, Glu^{134}–Leu^{140}; β3, Leu^{147}–Asp^{150}; β4, His^{154}–Ile^{157}; β5, Ser^{163}–Gln^{166}; β6, Gly^{183}–Tyr^{188}; and β7, Thr^{197}–Thr^{202}) and two α-helices (α1, Glu^{108}–Ser^{119}; α2, Arg^{211}–Glu^{230}). The seven β-strands are folded into two antiparallel β-sheets (β1-β4 and β5-β7), which are orthogonally arranged to form a β-sandwich structure that is closed off by the C-terminal α-helix (α2). These structural features are characteristic of the canonical PH domain fold (Fig. 7*A*), whereas the additional α-helix (α1) is tethered to the C-terminal α-helix (α2). A typical PH domain from PLC-δ1 complexed with Ins(1,4,5)P_3 (PDB code 1MAI) is presented in Fig. 7*B* as a reference. Inositol (1,4,5)-trisphosphate (Ins(1,4,5)P_3) binds to the positively charged surface (indicated by *blue* color) of the PH domain of PLC-δ1 and a corresponding positively charged surface is absent in the C-ter of ZF21.

DISCUSSION

Four *CXXC* sequences are conserved within the FYVE domain, as is the case with other zinc finger domains (49). In addition to the zinc finger motif, the FYVE domain comprises three additional conserved elements: the N-terminal W*XX*D, the central R(R/K)HHCR, and the C-terminal RVC sequences (49). These elements are conserved in the FYVE domain of ZF21, although the C-terminal RVC sequence is substituted by RQC. As we reported previously, the subcellular localization of ZF21 largely overlaps with that of EEA1, a well characterized endosomal marker, and substitution of the conserved His residues within the central R(R/K)HHCR motif of ZF21 to asparagine prevented its localization to endosomes (28). However, several studies have reported that the FYVE domain of EEA1 is essential but not sufficient for endosome targeting (29). Targeting of EEA1 to the endosome requires the presence of an additional ~40 amino acids N-terminal to the FYVE domain (29). Consistent with this observation, substitution of the FYVE domain of ZF21 with that of EEA1 abrogates the endosomal localization, leading to a diffuse cytoplasmic localization (Fig. 3*C*, m1V-SWAP, *green*). Unlike EEA1, ZF21 requires sequences C-terminal to the FYVE domain to localize to endosomes, because truncation of the C-ter region also leads to a pattern of diffuse cytoplasmic localization (Fig. 3*C*, m1V-N, *green*). Therefore, association of FYVE domain-containing proteins with lipid bilayers via the FYVE domain is likely affected by the nature of the surrounding protein sequences in a manner specific to each protein. In addition to PI(3)P, the FYVE domain of ZF21 binds FAK, whereas EEA1 does not. ZF21 also localizes to

the sites of FAs even though it has no FA-targeting motif (50). Therefore, the interaction of the FYVE domain of ZF21 with FAK is thought to be important for this localization. Indeed, expression of ZF21 could not promote cell migration of FAK-depleted cells and a ZF21 mutant that could not bind to FAK was unable to restore the migratory ability of ZF21-depleted cells. Thus, the FYVE domain of ZF21 is indispensable for its specific activity.

The C-ter of ZF21 also has a function independent from that of the FYVE domain, as it is sufficient to bind β-tubulin but not FAK. Structural analysis of the C-ter fragment by NMR spectroscopy and a structural similarity search using the Dali server (51) revealed that the C-ter domain shares structural homology with the PH domain of phospholipase C-β2 (PLC-β2) (PDB ID 2ZKM), with a *Z*-score of 9.8 and a sequence identity of 11%, and with that of phospholipase C-δ1 (PLC-δ1) (PDB code 1MAI), with a *Z*-score of 9.3 and a sequence identity of 13% (52, 53). PH domains exist in a number of proteins involved in signal transduction and in components of the cytoskeleton (31). Many PH domains bind phosphoinositides and are involved in membrane targeting. The PLC-δ1 PH domain tightly interacts with $Ins(1,4,5)P_3$, which is bound on the positively charged surface consisting of the β1/β2 and β3/β4 loops (Fig. 7*B*, *blue color area*) (53). The basic amino acid residues generating the positively charged surface in the PH domain make direct contact with the sugar phosphates of $Ins(1,4,5)P_3$. Site-directed mutagenesis of these residues markedly decreased the affinity of the PH domain for $Ins(1,4,5)P_3$ (54), indicating that the positively charged surface is essential to bind the phospholipid. These residues are also conserved and indispensable in other $Ins(1,4,5)P_3$-binding proteins, such as the phosphotyrosine-binding domain (55) or fructose-1,6-bisphosphate aldolase A (56). On the other hand, the corresponding surface of the ZF21 C-ter domain lacks such positively charged residues (Fig. 7*A*, *red color area*), suggesting that the ZF21 C-ter domain cannot bind phosphoinositides (Fig. 7*A*). However, confirmation of whether ZF21 indeed lacks affinity for phosphoinositides and whether the C-ter domain plays a role in the function of ZF21 via the PH-like domain will require the study of recombinant proteins with mutations within this region of the protein. The phosphotyrosine binding and the Enabled/VASP homology domains, which are members of the PH domain superfold family, are also used as interaction interfaces for protein ligands such as that of PLC-β2 (31, 57). Hence, it is particularly interesting how the C-ter domain of ZF21 interacts with β-tubulin.

The PH-like domain of ZF21 is sufficient to bind β-tubulin (27), but the role of this interaction in the function of ZF21 remains unclear. This is largely because of the fact that deletion of the PH-like domain also abolishes the ability of ZF21 to interact with intracellular vesicles via the FYVE domain. The FYVE domain and the PH-like domain of ZF21 may be functionally and/or conformationally interdependent *in vivo*. However, the interaction of ZF21 with β-tubulin must be important for the regulation of the disassembly of FAs, because β-tubulin is a component of microtubules that extend to FAs so as to trigger the disassembly (12). Kinesin motor proteins that convey vesicles to the cell periphery along with microtubules are also important for the regulation of the disassembly of FAs (16).

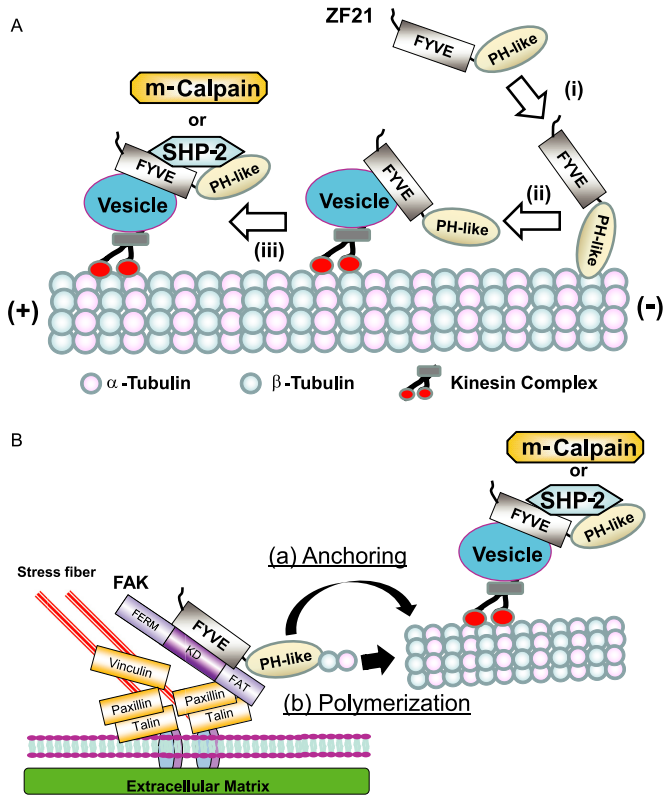

FIGURE 8. **Possible function of the PH-like domain of ZF21.** *A*, the PH-like domain of ZF21 may facilitate the loading of ZF21 onto transport vesicles localized to MTs and facilitates to convey the FA disassembly factors. Interaction of ZF21 with MTs via the PH-like domain and β-tubulin may represent an initial step of this process (*i*). ZF21 on MTs is thought to bind phosphoinositides within the transport vesicles (*ii*). ZF21 on MTs recruits FA disassembly factors, such as SHP-2 or m-calpain, to the transport vesicles (*iii*). The plus or minus end of MTs is indicated by symbols (+ or −), respectively. *B*, the PH-like domain of ZF21 may act as an acceptor site for MTs on FAs. MTs extended to FAs may be anchored to FAs by interacting with the PH-like domain of the ZF21 protein that already is localized to the FAs (*a*). ZF21 may recruit the heterodimeric α- and β-tubulin complex via the PH-like domain so as to provide substrates for the polymerization of MTs (*b*).

Therefore, the interaction of the PH-like domain of ZF21 with β-tubulin proteins comprising microtubules might facilitate the loading of ZF21 onto transport vesicles on microtubules (Fig. 8*A*). ZF21 also interacts with m-calpain and SHP-2, which might allow the former to convey these disassembly factors to FAs via microtubules (Fig. 8*A*). The PH-like and FYVE domains of ZF21 cooperate to bind these FA disassembly factors, whereas the interaction of ZF21 with FAK and β-tubulin only requires the FYVE or PH-like domain, respectively. Otherwise, the PH-like domain of ZF21 localized to FAs may act as an acceptor site for the plus end of microtubules (Fig. 8*B*, *a*). The exact mechanism might become more clear when the structural basis of the interaction between the PH-like domain and β-tubulin is solved. It is also possible that ZF21 binds a heterodimeric α- and β-tubulin complex via the PH-like domain so as to convey it along microtubules to the plus end where polymerization of tubulin is taking place (Fig. 8*B*, *b*). These possible functions of the PH-like domain of ZF21 are summarized in Fig. 8.

After we reported that ZF21 is a regulator of cell adhesion and migration, a separate report appeared that revealed that the expression of this gene (also termed MGC2550) is increased in metastatic colorectal cancer when compared with non-meta-

static disease, based on serial analysis of gene expression (30). Consistent with this finding in clinical specimens, ZF21 was confirmed to promote an early step of lung metastasis at least in an experimental metastasis assay in mice. The ability of ZF21 to promote cell migration through the ECM is presumably important for cancer cells to traverse blood vessels for extravasation and this idea is consistent with the fact that ZF21 knockdown rendered cells unable to invade into lung tissue. Cancer cells that failed to accomplish extravasation generally died within 24 h and were cleared rapidly from the bloodstream of lung tissue. However, increased expression of ZF21 in cancer cells promotes cell migration in, on the one hand, and reduces the ability of the cell to adhere to the ECM on the other. Therefore, overexpression of ZF21 in cancer cells may diminish survival signals evoked by the attachment to the ECM and enhance the rate of anoikis. Presumably, cancer cells use acquired resistance to apoptosis to antagonize the process of anoikis.

In conclusion, both the FYVE domain and the C-terminal PH-like domain are indispensable for prometastatic activity of ZF21. Thus, analysis of the structure of ZF21 provides important information to develop therapeutic agents to treat malignant tumors.

Acknowledgments—We thank Dr. Atsushi Miyawaki for kindly providing m1Venus cDNA clones, Dr. Takeharu Sakamoto for useful discussions, and Chieko Konishi and Tomoko Ando for excellent technical support.

REFERENCES

1. Avraamides, C. J., Garmy-Susini, B., and Varner, J. A. (2008) *Nat. Rev. Cancer* **8,** 604–617
2. Desgrosellier, J. S., and Cheresh, D. A. (2010) *Nat. Rev. Cancer* **10,** 9–22
3. Meighan, C. M., and Schwarzbauer, J. E. (2008) *Curr. Opin. Cell Biol.* **20,** 520–524
4. Truong, H., and Danen, E. H. (2009) *Cell Adh. Migr.* **3,** 179–181
5. Hynes, R. O. (2002) *Cell* **110,** 673–687
6. Liu, S., Calderwood, D. A., and Ginsberg, M. H. (2000) *J. Cell Sci.* **113,** 3563–3571
7. Geiger, B., Bershadsky, A., Pankov, R., and Yamada, K. M. (2001) *Nat. Rev. Mol. Cell Biol.* **2,** 793–805
8. Mitra, S. K., Hanson, D. A., and Schlaepfer, D. D. (2005) *Nat. Rev. Mol. Cell Biol.* **6,** 56–68
9. Mitra, S. K., and Schlaepfer, D. D. (2006) *Curr. Opin. Cell Biol.* **18,** 516–523
10. Critchley, D. R. (2000) *Curr. Opin. Cell Biol.* **12,** 133–139
11. Humphries, J. D., Wang, P., Streuli, C., Geiger, B., Humphries, M. J., and Ballestrem, C. (2007) *J. Cell Biol.* **179,** 1043–1057
12. Ezratty, E. J., Partridge, M. A., and Gundersen, G. G. (2005) *Nat. Cell Biol.* **7,** 581–590
13. Webb, D. J., Donais, K., Whitmore, L. A., Thomas, S. M., Turner, C. E., Parsons, J. T., and Horwitz, A. F. (2004) *Nat. Cell Biol.* **6,** 154–161
14. Webb, D. J., Parsons, J. T., and Horwitz, A. F. (2002) *Nat. Cell Biol.* **4,** E97–100
15. Kaverina, I., Krylyshkina, O., and Small, J. V. (1999) *J. Cell Biol.* **146,** 1033–1044
16. Krylyshkina, O., Kaverina, I., Kranewitter, W., Steffen, W., Alonso, M. C., Cross, R. A., and Small, J. V. (2002) *J. Cell Biol.* **156,** 349–359
17. Glading, A., Lauffenburger, D. A., and Wells, A. (2002) *Trends Cell Biol.* **12,** 46–54
18. Angers-Loustau, A., Côté, J. F., Charest, A., Dowbenko, D., Spencer, S., Lasky, L. A., and Tremblay, M. L. (1999) *J. Cell Biol.* **144,** 1019–1031
19. Yu, D. H., Qu, C. K., Henegariu, O., Lu, X., and Feng, G. S. (1998) *J. Biol. Chem.* **273,** 21125–21131
20. Zhang, Z., Lin, S. Y., Neel, B. G., and Haimovich, B. (2006) *J. Biol. Chem.* **281,** 1746–1754
21. Uekita, T., Gotoh, I., Kinoshita, T., Itoh, Y., Sato, H., Shiomi, T., Okada, Y., and Seiki, M. (2004) *J. Biol. Chem.* **279,** 12734–12743
22. Niiya, D., Egawa, N., Sakamoto, T., Kikkawa, Y., Shinkawa, T., Isobe, T., Koshikawa, N., and Seiki, M. (2009) *J. Biol. Chem.* **284,** 27360–27369
23. Sakamoto, T., and Seiki, M. (2009) *J. Biol. Chem.* **284,** 30350–30359
24. Tomari, T., Koshikawa, N., Uematsu, T., Shinkawa, T., Hoshino, D., Egawa, N., Isobe, T., and Seiki, M. (2009) *Cancer Sci.* **100,** 1284–1290
25. Sakamoto, T., and Seiki, M. (2010) *J. Biol. Chem.* **285,** 29951–29964
26. Hoshino, D., Tomari, T., Nagano, M., Koshikawa, N., and Seiki, M. (2009) *J. Biol. Chem.* **284,** 27315–27326
27. Nagano, M., Hoshino, D., Sakamoto, T., Akizawa, T., Koshikawa, N., and Seiki, M. (2010) *Cell. Adh. Migr.* **5,** 23–28
28. Nagano, M., Hoshino, D., Sakamoto, T., Kawasaki, N., Koshikawa, N., and Seiki, M. (2010) *J. Biol. Chem.* **285,** 21013–21022
29. Stenmark, H., Aasland, R., Toh, B. H., and D'Arrigo, A. (1996) *J. Biol. Chem.* **271,** 24048–24054
30. Saha, S., Bardelli, A., Buckhaults, P., Velculescu, V. E., Rago, C., St. Croix, B., Romans, K. E., Choti, M. A., Lengauer, C., Kinzler, K. W., and Vogelstein, B. (2001) *Science* **294,** 1343–1346
31. Blomberg, N., Baraldi, E., Nilges, M., and Saraste, M. (1999) *Trends Biochem. Sci.* **24,** 441–445
32. Yabuki, T., Motoda, Y., Hanada, K., Nunokawa, E., Saito, M., Seki, E., Inoue, M., Kigawa, T., and Yokoyama, S. (2007) *J. Struct. Funct. Genomics* **8,** 173–191
33. Kigawa, T., Yabuki, T., Yoshida, Y., Tsutsui, M., Ito, Y., Shibata, T., and Yokoyama, S. (1999) *FEBS Lett.* **442,** 15–19
34. Yokoyama, S., Hirota, H., Kigawa, T., Yabuki, T., Shirouzu, M., Terada, T., Ito, Y., Matsuo, Y., Kuroda, Y., Nishimura, Y., Kyogoku, Y., Miki, K., Masui, R., and Kuramitsu, S. (2000) *Nat. Struct. Biol.* **7,** (suppl.) 943–945
35. Li, H., Koshiba, S., Hayashi, F., Tochio, N., Tomizawa, T., Kasai, T., Yabuki, T., Motoda, Y., Harada, T., Watanabe, S., Inoue, M., Hayashizaki, Y., Tanaka, A., Kigawa, T., and Yokoyama, S. (2008) *J. Biol. Chem.* **283,** 27165–27178
36. Delaglio, F., Grzesiek, S., Vuister, G. W., Zhu, G., Pfeifer, J., and Bax, A. (1995) *J. Biomol. NMR* **6,** 277–293
37. Johnson, B. A., and Blevins, R. A. (1994) *J. Biomol. NMR* **4,** 603–614
38. Kobayashi, N., Iwahara, J., Koshiba, S., Tomizawa, T., Tochio, N., Güntert, P., Kigawa, T., and Yokoyama, S. (2007) *J. Biomol. NMR* **39,** 31–52
39. Güntert, P. (2004) *Methods Mol. Biol.* **278,** 353–378
40. Herrmann, T., Güntert, P., and Wüthrich, K. (2002) *J. Mol. Biol.* **319,** 209–227
41. Cornilescu, G., Delaglio, F., and Bax, A. (1999) *J. Biomol. NMR* **13,** 289–302
42. Laskowski, R. A., Rullmannn, J. A., MacArthur, M. W., Kaptein, R., and Thornton, J. M. (1996) *J. Biomol. NMR* **8,** 477–486
43. Koradi, R., Billeter, M., and Wuthrich, K. (1996) *J. Mol. Graph.* **14,** 51–55
44. Pinner, S., and Sahai, E. (2008) *Nat. Cell Biol.* **10,** 127–137
45. Medjkane, S., Perez-Sanchez, C., Gaggioli, C., Sahai, E., and Treisman, R. (2009) *Nat. Cell Biol.* **11,** 257–268
46. Dumas, J. J., Merithew, E., Sudharshan, E., Rajamani, D., Hayes, S., Lawe, D., Corvera, S., and Lambright, D. G. (2001) *Mol. Cell* **8,** 947–958
47. Kutateladze, T. G., Ogburn, K. D., Watson, W. T., de Beer, T., Emr, S. D., Burd, C. G., and Overduin, M. (1999) *Mol. Cell* **3,** 805–811
48. Finn, R. D., Mistry, J., Tate, J., Coggill, P., Heger, A., Pollington, J. E., Gavin, O. L., Gunasekaran, P., Ceric, G., Forslund, K., Holm, L., Sonnhammer, E. L., Eddy, S. R., and Bateman, A. (2010) *Nucleic Acids Res.* **38,** D211–D222
49. Gillooly, D. J., Simonsen, A., and Stenmark, H. (2001) *Biochem. J.* **355,** 249–258
50. Shen, Y., and Schaller, M. D. (1999) *Mol. Biol. Cell* **10,** 2507–2518
51. Holm, L., and Park, J. (2000) *Bioinformatics* **16,** 566–567
52. Hicks, S. N., Jezyk, M. R., Gershburg, S., Seifert, J. P., Harden, T. K., and Sondek, J. (2008) *Mol. Cell.* **31,** 383–394

53. Ferguson, K. M., Lemmon, M. A., Schlessinger, J., and Sigler, P. B. (1995) *Cell* **83,** 1037–1046
54. Yagisawa, H., Sakuma, K., Paterson, H. F., Cheung, R., Allen, V., Hirata, H., Watanabe, Y., Hirata, M., Williams, R. L., and Katan, M. (1998) *J. Biol. Chem.* **273,** 417–424
55. Takeuchi, H., Matsuda, M., Yamamoto, T., Kanematsu, T., Kikkawa, U., Yagisawa, H., Watanabe, Y., and Hirata, M. (1998) *Biochem. J.* **334,** 211–218
56. Baron, C. B., Tolan, D. R., Choi, K. H., and Coburn, R. F. (1999) *Biochem. J.* **341,** 805–812
57. Lemmon, M. A. (2004) *Biochem. Soc. Trans.* **32,** 707–711
58. Nicholls, A., Sharp, K. A., and Honig, B. (1991) *Proteins* **11,** 281–296